

1 **Centennial scale benthic foraminiferal record of late Holocene**
2 **oceanographic variability in Disko Bugt, West Greenland**

3 K. Perner^{1*}; M. Moros^{1,2}; J.M. Lloyd³; A. Kuijpers⁴; R.J. Telford^{2,5}; J. Harff^{1,6}

4

5 1 Institute for Baltic Sea Research Warnemuende, Department of Marine Geology,
6 Germany

7 2 Bjerknes Centre for Climate Research, Norway

8 3 Durham University, Department of Geography, UK

9 4 Geological Survey of Denmark and Greenland, Copenhagen, Denmark

10 5 Department of Biology, University of Bergen, Norway

11 6 University of Szczecin, Institute of Marine and Coastal Sciences, Poland

12

13 Keywords: Late Holocene, benthic foraminifera, West Greenland Current, East
14 Greenland Current, Irminger Current, NAO

15 *Corresponding author: kerstin.perner@io-warnemuende.de

16

17

18

19 **Abstract:**

20 We present a new centennial to decadal scale benthic foraminiferal record of
21 late Holocene climate variability and oceanographic changes off West Greenland.
22 The investigated site from southwest Disko Bugt highlights substantial subsurface
23 water mass changes (e.g. temperature and salinity) of the West Greenland Current
24 (WGC) over the past 3.6 ka BP. Benthic foraminifera reveal a long-term late Holocene
25 cooling trend, which may be attributed to increased advection of cold, low salinity

26 water masses derived from the East Greenland Current (EGC). Cooling becomes
27 most pronounced from c. 1.7 ka BP onwards, as the calcareous Atlantic benthic
28 foraminiferal fauna decreased significantly, while being replaced by an agglutinated
29 Arctic fauna. Superimposed on this cooling trend, centennial scale variability in the
30 WGC reveals a marked cold phase at c. 2.5 ka BP, which may correspond to the 2.7
31 ka BP cooling-event recorded in marine and terrestrial archives elsewhere in the
32 North Atlantic region. A warm phase recognized at c. 1.8 ka BP is likely to
33 correspond to the 'Roman Warm Period' and represents the warmest bottom water
34 conditions recorded in Disko Bugt during the last 3.6 ka BP. During the time period of
35 the 'Medieval Climate Anomaly' we observe only a slight warming of the WGC. A
36 progressively more dominant cold water contribution from the EGC on the WGC is
37 documented by the prominent rise in abundance of agglutinated Arctic water species
38 from 0.9 ka BP onwards, which culminates at c. 0.3 ka BP. This cooling event
39 represents the coldest episode of the 'Little Ice Age'.

40 Gradually increased influence of cold low salinity water masses derived from
41 the EGC may be linked to enhanced advection of Polar and Arctic water by the EGC.
42 These changes are possibly associated with a reported shift in the large-scale North
43 Atlantic Oscillation atmospheric circulation pattern towards a more frequent negative
44 North Atlantic Oscillation mode during the late Holocene.

45

46

47 **1. Introduction**

48 The Disko Bugt area in central West Greenland (Fig.1) is linked to the large-
49 scale North Atlantic current system and climate variability via the West Greenland
50 Current (WGC). The relative influence of Atlantic (e.g. Irminger Current) vs. Arctic
51 (e.g. East Greenland Current) derived water masses within the WGC determines the

52 hydrographic conditions off West Greenland with significant impact on the benthic
53 foraminiferal fauna. Previous studies reported postglacial re-appearance of the WGC
54 in the Disko Bugt area from c. 9 to 10 ka BP, based on mollusc, dinocyst and
55 foraminifera data (e.g. Kelly, 1979 and 1985; Ostermann and Nelson, 1989, Feyling-
56 Hanssen and Funder, 1990; Funder and Weidick, 1991; Lloyd et al., 2005). Cooling
57 is reported from c. 5 ka BP in Disko Bugt, possibly associated with Neoglacial cooling
58 identified throughout much of western Greenland (Kelly, 1980; Dahl-Jensen et al.,
59 1998; Kaufman et al., 2004). A variety of studies from Disko Bugt and the West
60 Greenland margin document increased temperature and salinity variability in the
61 WGC during the late Holocene (Lassen et al., 2004; Lloyd, 2006a,b; Lloyd et al.,
62 2007; Møller et al., 2006; Moros et al., 2006b; Lloyd et al., 2007; Seidenkrantz et al.,
63 2007, 2008; Krawczyk et al., 2010). In addition, WGC temperature changes on a
64 multi decadal timescale has been noted to have a profound impact on subsurface
65 melting of Disko Bugt outlet glaciers (e.g. Jakobshavn Isbræ), at least during the last
66 60 years (Holland et al., 2008; Rignot et al., 2010; Lloyd et al., 2011).

67 One proxy method to investigate changes in ocean current properties is to
68 study benthic foraminifera. Their faunal diversity and species distribution is highly
69 dependent on ecological parameters (Murray, 1991). The distribution of certain
70 species, particularly in high arctic environments, is strongly controlled by water mass
71 characteristics, such as temperature and salinity (e.g. Rytter et al., 2002; Sejrup et
72 al., 2004) and surface water productivity (i.e. food supply). This close relationship has
73 been well documented in a number of benthic foraminiferal studies from west and
74 south Greenland (e.g. Lassen et al., 2004; Lloyd, 2006a,b; Seidenkrantz et al., 2007),
75 the Baffin Bay area (e.g. Schröder-Adams et al., 1990; Schafer and Cole, 1986),
76 fjords along the East Greenland margin and fjords and in the northern North Atlantic

77 region, including Iceland (e.g. Jennings and Helgadottir, 1994; Andrews et al., 2001;
78 Jennings et al., 2002) and Svalbard (e.g. Hald and Steinsund, 1992).

79 In the present study a new marine sediment core from south-western Disko
80 Bugt is used for high-resolution paleoenvironmental reconstruction to elucidate
81 qualitative changes in bottom water mass properties of the WGC through the late
82 Holocene (since 3.6 ka BP). We use benthic foraminifera to achieve this aim, which
83 provide now a highly detailed picture of late Holocene oceanographic evolution in
84 West Greenland (i.e. WGC property changes). In addition, our data will allow
85 investigation of the link between oceanographic changes off West Greenland and
86 North Atlantic circulation changes as recorded in other marine and terrestrial records
87 in the North Atlantic region.

88

89

90 **2. Study area and oceanographic setting**

91 Disko Bugt, located in central West Greenland, is a large marine embayment
92 (Fig.1). The topography of the area is characterized by a rugged sea bed with
93 relatively shallow water depths, typically varying between 200 and 400 m. Maximum
94 water depths of up to 990 m occur in the deep water trough, 'Egedesminde Dyb' (Fig.
95 1). The Egedesminde Dyb channel has a glacial origin and continues to the shelf
96 edge where a large trough-mouth fan is found (Zarudzki, 1980). CTD data from Disko
97 Bugt (Andresen, 1981; Buch, 1981; Buch et al., 2004; Lloyd et al., 2006) show that
98 the WGC (3.5–4 °C, 34.2–34.4 PSU) forms the bottom waters in the bay. Surface
99 waters, in contrast, are influenced by fresh-meltwater flux from land, icebergs and the
100 previous season's pack ice as well as relatively low-salinity polar surface water
101 advected from Baffin Bay. Temperature and salinity profiles along a transect from
102 south-west to central Disko Bugt show that the WGC constitutes the water mass

103 below *c.* 150 m water depth (Harff et al., 2007). Further Andresen (1981) found no
104 indications of an admixture of deep Baffin Bay waters below 300 m water depth,
105 penetrating into Disko Bugt. The WGC constitutes a mixture of the following water
106 masses: Atlantic-sourced relatively warm and saline water from the North Atlantic
107 Irminger Current (IC), a side branch of the North Atlantic Current (NAC); Arctic-
108 sourced cold, low-salinity water from the East Greenland Current (EGC) (Buch,
109 1981); and local meltwater discharge into the WGC along the SW Greenland coast
110 (see Fig.1). The WGC enters Disko Bugt from the southwest and flows northwards
111 exiting primarily through the Vaigat into Baffin Bay. A branch of the WGC is deflected
112 into Baffin Bay in an anticyclonic gyre west of Disko Island, while the remainder of the
113 WGC continues to flow northward into northern Baffin Bay (Andresen, 1981;
114 Humlum, 1999; Bâcle et al., 2002). Recent studies show that the WGC also
115 penetrates the deeper parts of the fjords in Disko Bugt, for example Jacobshavn
116 Isfjord and Torssukatak (Holland et al., 2008; Rignot et al., 2010). The presence of
117 the WGC in Disko Bugt has a significant impact on the distribution of agglutinated
118 and calcareous benthic foraminifera (Lloyd et al., 2006b; Lloyd et al., 2011). The
119 study site investigated here reflects open-marine environmental conditions rather
120 than glaciomarine, as sedimentation in Egedesminde Dyb is linked to current activity.

121

122

123 **3. Material and Methods**

124 **3.1 Sediment sampling**

125 Sediments were collected from site MSM 343310 (68°38'861N,
126 53°49'493W, Fig. 1) by using a multi and a gravity core in the deep-water trough
127 Egedesminde Dyb, south-western Disko Bugt (water depth: 855 m) during cruise
128 MSM05/03 of the *R/V "Maria S. Merian"* (Harff et al., 2007). The multi core (length: 32

129 cm) was sampled in 0.5 cm and the gravity core (length: 939 cm) in 1 cm intervals
130 and stored at 4°C in a cold storage facility.

131

132 **3.2 Chronology**

133 Age control is provided by accelerator mass spectrometry AMS ¹⁴C dates on
134 mollusc shells and benthic foraminifera (Table 1, Fig. 2). The chronology of the multi
135 core is based on 10 AMS ¹⁴C dates, ²¹⁰Pb/¹³⁷Cs measurements and other
136 chronological evidence (Lloyd et al., 2011). The chronology of the gravity core is
137 based on 20 AMS ¹⁴C dates. AMS radiocarbon dates were calibrated with the
138 Marine09 (Reimer et al., 2009) calibration curve using OxCal 4.1 (Bronk Ramsey,
139 2009). The marine reservoir offset was estimated using the marine reservoir age
140 database of Reimer and Reimer (2001). This database includes six entries for Disko
141 Bugt from bivalves (*Mytilus edulis* and *Astarte montagui*) and seal bones (Krog and
142 Tauber, 1974; Tauber 1979; McNeely et al., 2006). Most of these samples are from
143 shallow water, so we use the larger and more precise ΔR of 140 ± 30 years, than the
144 smaller ΔR of two measurements on *Astarte* collected in 60-70m water (McNeely et
145 al., 2006). An age model was fitted to the calibrated ¹⁴C using mixed effect modeling
146 (Heegaard et al., 2005).

147

148 **3.3 Foraminiferal sample processing**

149 For foraminiferal analysis of the calcareous and agglutinated fauna, a standard
150 volume of 5 ml sediment was soaked in deionized water overnight and sieved at 63
151 μm just before counting. The multi core was counted at 0.5 cm intervals and gravity
152 core at 4 cm intervals. Foraminifera were counted from the wet residue >63 μm to
153 reduce the loss of the more fragile arenaceous species caused by drying out of
154 sediment. More than 350 benthic foraminiferal specimens were counted per sample,

155 on a squared picking tray and identified to species level under a stereomicroscope.
156 Planktonic foraminifera, all *Neogloboquadrina pachyderma* (sin.), were also picked
157 and identified from the 63 μm fraction. However, abundance of *N. pachyderma* is
158 very low (<1 %) and therefore not included in the following discussion.

159

160

161 **4. Results**

162 **4.1 Lithology**

163 Sediments from site 343310 are composed of moderate olive brown to olive
164 gray mottled organic rich silty clay. The total organic carbon content is on average
165 2.8%. The sand content (fraction >63 μm) of the sediment is relatively low and
166 averages c. 4% of dry weight. X-radiograph analysis revealed that only a small
167 quantity of ice-rafted detritus (IRD) occurs in the sediments. Further, no turbidites are
168 observed in the record.

169

170 **4.2 Age models**

171 The age model reveals a high and almost linear sedimentation rate of 3.5 mm
172 per year (Fig. 2). Hence, our sample resolution of 4 cm allows the proxies to be
173 resolved at decadal scale (12-15 years, Fig. 2). According to our age models the
174 multi core and gravity core do not overlap. The composite record shows a gap of
175 approximately 100 years, which is due to the gravity core coring technique. Parallel
176 dating of mollusc shells and benthic foraminifera from same depth intervals revealed
177 no divergence between respective AMS ^{14}C dates as variation is within the error (see
178 Table 1). The applied ΔR of 140 ± 30 years (Lloyd et al., 2011) represents the
179 modern day value in Disko Bugt, as the water mass composition of the WGC is
180 predominantly influenced by the EGC. This ΔR fits with the reported range of ΔR of

181 130 to 115 ± 25 years for the EGC (Tauber and Funder, 1975). Because of the
182 variable influence of the EGC on WGC water mass properties through time (see
183 following discussion) we are aware of possible variations in ΔR with time, which
184 should be considered when comparing our results to other records/ events in the
185 North Atlantic region.

186

187 **4.3 Benthic foraminifera**

188 **4.3.1 General faunal characteristics**

189 A total of 53 benthic foraminiferal species were identified: 20 agglutinated and
190 33 calcareous taxa. A complete list of identified species is given in appendix A.1. An
191 average of 30 species was identified and species abundance averages 150
192 specimens per ml of wet sediment per sample. We find good preservation of
193 agglutinated and calcareous taxa and only minimal evidence of post mortem
194 (dissolution) changes, supported by low numbers of counted test linings per sample
195 (Fig. 3). The total benthic foraminiferal fauna is characterized by high abundance of
196 *Cuneata arctica*, *Deuterammia ochracea*, *Eggerella advena* and *Spiroplectammina*
197 *biformis* (agglutinated taxa) and by *Cassidulina reniforme*, *Elphidium excavatum*
198 *forma clavata*, *Islandiella norcrossi* and *Nonionellina labradorica* (calcareous taxa,
199 see Fig. 3).

200 To address and identify changes in water mass characteristics of the WGC,
201 we use summary curves of benthic foraminifera based on their ecological tolerance
202 (associated directly or indirectly with temperature and salinity). We use a chilled
203 Atlantic water group (AtlW), including relative warm water taxa and an Arctic water
204 group (AW), including relatively cold water taxa (see Table 2). Atlantic water
205 indicators are: *Cassidulina reniforme*, *Islandiella norcrossi*, *Pullenia osloensis*,
206 *Cassidulina neoteretis* (calcareous species), and *Adercotryma glomerata*,

207 *Ammoscalaria pseudospiralis*, *Reophax fusiformis* and *Reophax pilulifer*
208 (agglutinated species). These species are often reported from fjord and shelf areas
209 associated with Atlantic water influence (Vilks, 1981; Mudie et al., 1984; Mackensen
210 et al., 1985; Jennings and Helgadottir, 1994; Hald and Steinsund, 1996; Hald and
211 Korsun, 1997; Duplessy et al., 2001; Wollenburg et al., 2004; Lloyd 2006a). The
212 species *C. reniforme* is often associated with glaciomarine conditions from relatively
213 shallow and glacially influenced fjords (e.g. Nagy, 1965; Elverhøi et al., 1980;
214 Ostermann and Nelson, 1989; Vilks, 1989; Jennings and Helgadottir, 1994; Hansen
215 and Knudsen, 1995; Hald and Korsun, 1997, Lloyd, 2005). However, we include *C.*
216 *reniforme* in the Atlantic group, which has been associated with chilled Atlantic water
217 (e.g. Hald and Steinsund 1996). This is supported by the context of our study, as the
218 site investigated here is from a deep-water trough (855 m water depth) in relatively
219 open water conditions (relatively high TOC content, average of 2.8%) under the direct
220 influence of the WGC (Atlantic sourced water) and approximately 100 km from
221 modern tidewater glaciers in the fjords of Disko Bugt. Importantly the site is not
222 subjected to any direct melt water discharge from the Greenland Ice Sheet during the
223 late Holocene (Andresen, 1981; Buch, 1981; Buch et al., 2004; Lloyd et al., 2006a).

224 The Arctic water group (Table 2) includes *Stainforthia feylingi*, *Elphidium*
225 *excavatum* f. *clavata* and *Islandiella helenae* (calcareous taxa) and *Cuneata arctica*,
226 *Spiroplectammina biformis* and *Recurvoides turbinatus* (agglutinated taxa). *Elphidium*
227 *excavatum* f. *clavata*, a known opportunistic species, is able to tolerate relatively
228 unstable and colder environmental conditions (e.g. variability in food supply, salinity
229 and temperature) (Ostermann and Nelson, 1989; Vilks et al., 1989; Hald et al., 1994;
230 Hald and Korsun, 1997). This species is also found in high abundance (up to 30% of
231 the total assemblage) in certain intervals, which cannot be linked to any direct
232 meltwater discharge, and hence we cannot consider *E. excavatum* f. *clavata* as a

233 glaciomarine species in this context, though we classify it as a AW indicator in terms
234 of representing relatively harsh and variable environmental conditions. *Stainforthia*
235 *feylingi* is described by Knudsen and Seidenkrantz (1994) as indicative and tolerant
236 of unstable environmental conditions. There is generally poor knowledge of the
237 environmental controls on *S. feylingi*. Species of the genus *Stainforthia* are
238 commonly recorded in areas of very harsh, limiting ecological conditions, often with
239 only episodic food supply, variable salinity levels and anoxic conditions when most
240 species are unable to survive/ compete (Alve, 1994; Bernhard and Alve, 1996;
241 Knudsen and Seidenkrantz, 1994; Rasmussen et al., 2002). Polyak and Solheim
242 (1994) and Steinsund et al. (1994) link relatively high abundance of *I. helenae* to
243 summer ice-edge productivity in areas of seasonal ice cover in the Barents Sea.
244 *Cuneata arctica* and *S. biformis* are associated with cold less saline or arctic sourced
245 waters (Williamson et al., 1984; Schafer and Cole, 1986; Alve, 1990, 1991; Jennings
246 and Helgadottir, 1994; Madsen and Knudsen, 1994; Korsun and Hald, 1998;
247 Jennings et al., 2001).

248 In our record we use the calcareous AtIW species (AtIWcalc) as the 'warm end
249 member' assemblage, representing the NAC/IC influence on the WGC, whereas
250 agglutinated AW species (AWagg) are the 'cold end member' assemblage,
251 representing predominant EGC influence. A subdivision of our benthic foraminiferal
252 record into 4 zones (A-D) is based on distinct changes in the combined percentage
253 abundance of agglutinated and calcareous species; the ratio of calcareous vs.
254 agglutinated specimens (Fig.3) and is supported by the distribution of AtIW and AW
255 indicator species (Tab. 2).

256 The calculated ratio of calcareous vs. agglutinated specimens reveals marked
257 shifts from a predominantly calcareous to agglutinated fauna through the last 3.6 ka
258 BP (Fig. 3). We find highest abundance of calcareous foraminifera in zones A and C,

259 forming up to 70 % of the total assemblage. By contrast, agglutinated foraminifera
260 form up to 80 % of the total assemblage in zones B and D. Therefore, a more
261 detailed consideration of the agglutinated and calcareous fauna is useful. The high
262 abundance of total foraminifera (>100 specimens per ml sediment) allows this.
263 Accordingly, percentage calculations for agglutinated and calcareous species were
264 made separately and are presented in Fig. 4 (agglutinated species) and Fig. 5
265 (calcareous species). In the following sections the faunal composition of zones A-D is
266 presented separately for the calcareous and agglutinated species.

267

268 **4.3.2 Agglutinated species distribution**

269 The Assemblage zone A (3.6 to c. 2.6 ka BP) is characterized by high
270 abundance of *Deuterammina ochracea* (mean 40%) and *Eggerella advena* (mean
271 35%). From 2.6 to c. 1.9 ka BP (zone B) the abundance of AWagg species is below
272 20%. An increase of AWagg species *C. arctica* (15%) and *S. biformis* (10%) is seen
273 in this interval. Notable peak abundance of *R. turbinatus* (up to 20%), is found at c.
274 2.4 and 2.1 ka BP (see Fig. 4). Lowest percentage abundance of total agglutinated
275 species is found between 1.9 and 1.7 ka BP (zone C, see Fig.4). By 1.3 ka BP
276 AWagg species (*C. arctica* and *S. biformis*) become more important and reach a
277 maximum of c. 45% by 0.9 ka BP. A rise in AtIWagg species (up to c. 10%, Fig. 4) is
278 noted from 1.5 ka BP onwards. In assemblage zone D (0.9 ka BP to the present) we
279 find a major increase of AWagg species *C. arctica* (average 35%) and *S. biformis*
280 (average 20%) with maximum abundance at 0.3 ka BP is found (see Fig. 4). We also
281 note a prominent rise in abundance of *Textularia torquata* (>10%) and *R. turbinatus*
282 (up to 10%). AtIW species *R. fusiformis* (12 %) along with lower levels of *Reophax*
283 *pilulifer* (6%) become an important component of the assemblage over the last
284 century (Fig. 4).

285

286 **4.3.3 Calcareous species distribution**

287 From 3.6 to c. 2.6 ka BP (zone A) we find a calcareous fauna, which is
288 dominated by the AtIWcalc species *C. reniforme* and *I. norcrossi*, with maximum
289 abundance of 60% at 3.2 ka BP. The infaunal species *N. labradorica* averages 20%
290 in this zone. A relatively high abundance of *E. excavatum* f. *clavata* is found, with a
291 distinct drop in abundance from c. 40% to below 5% seen at c. 3.5 and 3.0 ka BP
292 (Fig. 5). In assemblage zone B (2.6 to 1.9 ka BP) AtIWcalc species average 30% and
293 decrease to c. 20% at c. 2.5 ka BP, driven by a pronounced drop in abundance of *C.*
294 *reniforme* (10% at 2.5 ka BP, Fig. 5). In this interval AWcalc species *E. excavatum* f.
295 *clavata* fluctuates markedly in abundance and at 2.7 ka BP and 2.4 ka BP a peak of
296 c. 40% is found. Detritus feeder *N. labradorica* averages c. 20%, with notably low
297 abundance (below 10%) at c. 2.5 ka BP (see Fig. 5). In zone C (1.9 to 0.9 ka BP) we
298 record marked changes in the calcareous fauna. From 1.9 to 1.7 ka BP AtIWcalc
299 species dominate the calcareous assemblage (up to 50%), accompanied by high
300 abundance of *N. labradorica* (25%) and *G. auriculata arctica* (30%, see Fig. 5).
301 Relatively low abundance of AWcalc species *E. excavatum* f. *clavata* (~5%) is
302 recorded from 1.9 to 1.6 ka BP. From 1.5 ka BP a pronounced rise in abundance of
303 *E. excavatum* f. *clavata* (up to 30%) is seen alongside a gradual fall at 1.0 ka BP in
304 the abundance of AtIWcalc species, which average c. 25% from 1.5 to 0.9 ka BP.
305 From 0.9 ka BP onwards (zone D) we record a sharp change in the calcareous
306 assemblage. A notable decrease in abundance of AtIWcalc species *C. reniforme* and
307 *I. norcrossi* at 0.9 ka BP and calcAW species *E. excavatum* f. *clavata* down to c. 5%
308 is seen at 0.7 ka BP. These species are replaced by a major rise in abundance of
309 AWcalc species *S. feylingi* up to 40%, with a large spike at 0.3 ka BP (see Figs. 3
310 and 5). Additionally, we find increasing abundance of *I. helenae* (5%) during this

311 interval. Detritus feeder such as *N. labradorica*, *G. auriculata arctica* and *B.*
312 *pseudopunctata* still represent about 30% of the calcareous assemblage (Fig. 5), but
313 show low abundance at 0.3 ka BP.

314

315

316 **5. Discussion**

317 **5.1 Long-term late Holocene cooling and paleoceanographic implications**

318 Our new high-resolution benthic foraminiferal record from Disko Bugt
319 documents a marked long-term cooling trend over the last 3.6 ka BP. This trend is
320 clearly seen in the percentage decrease of the chilled Atlantic Water species *C.*
321 *reniforme* (see Figs. 3, 4 and 5) and average increase of AWagg indicators, reflecting
322 the gradually increased influence of the EGC within the WGC over the late Holocene.
323 Trends we recognized in AtIWcalc and AWagg indicators show cooling becomes
324 most pronounced from c. 1.7 ka BP onwards, as AtIWcalc species decrease
325 significantly and AWagg species increase notably (Fig. 6). We suggest that this
326 cooling is a consequence of increasing EGC influence on the water mass
327 composition of the WGC. This agrees with studies from the Denmark Strait and from
328 the SE Greenland margin, documenting an expansion and intensification of the EGC
329 during the late Holocene (Kuijpers et al., 2003; Jennings et al., 2011). Jennings et al.
330 (2011) report a predominant agglutinated fauna, marking the strong EGC influence
331 from the Denmark Strait from 3.3 ka BP. Further studies reported an increased
332 contribution of colder/fresher arctic water masses and increased drift ice within the
333 EGC from c. 5.0 ka BP (Andrews et al., 1997; Eiríksson et al., 2004; Moros et al.,
334 2006a). From c. 0.9 ka BP onwards, we find this influence to be more persistent and
335 intense, as a dominant agglutinated fauna is established and peak abundance of
336 AWagg species mark the culmination of the cooling trend at c. 0.3 ka BP during the

337 Little Ice Age (LIA). Longer-term late Holocene cooling is recognized in a variety of
338 marine (Jennings et al., 2002; Andersson et al., 2003; Risebrobakken et al., 2003;
339 Giraudeau et al., 2004; Eiríksson et al., 2004; Hall et al., 2004; Moros et al., 2004; de
340 Vernal and Hillarie Marcel, 2006; Kaufmann et al., 2009; Ólafsdóttir et al., 2010) and
341 terrestrial arctic temperature proxy data from the North Atlantic region (e.g. Alley et
342 al., 1999; Kaufman et al., 2009, see Fig. 6d, e).

343

344 **5.2 Millennial to centennial scale variability in subsurface waters of the** 345 **WGC**

346 Superimposed on the longer-term late Holocene cooling trend we identify
347 millennial to centennial scale variability in Disko Bugt bottom waters since 3.6 ka BP.
348 The basal part of the record, Zone A - spanning the interval 3.6 to 2.6 ka BP, is
349 characterized by high abundance of AtIWcalc species (Fig. 6c). Hence, we infer
350 warmer bottom water conditions prevailing in Egedesminde Dyb and accordingly a
351 relatively strong influence of the NAC/IC. This assumption is supported by a relative
352 low abundance of AWagg species (Fig. 6b). The occurrence of detritus feeder's *N.*
353 *labradorica* and *G. auriculata arctica* (Schafer and Cole, 1986; Corliss and Chen,
354 1988; Corliss, 1991; Rytter et al., 2002; Jennings et al., 2004, see Fig. 5) reflects
355 relatively high food availability and supply of phytodetritus to the seafloor during this
356 interval. The warm WGC corresponds to relatively high and stable air temperatures
357 over the Greenland ice cap (Alley et al., 1999, Fig. 6e) and is associated with
358 enhanced meltwater production as demonstrated in sediment core records from
359 Ammarilik fjord, West Greenland (e.g. Møller et al. 2006).

360 We recognize a marked change to relatively colder oceanographic conditions
361 off West Greenland in the 2.6 to 1.9 ka BP interval (Zone B). The prominent rise in
362 agglutinated AW species at c. 2.4 - 2.5 ka BP, reflects cooling and freshening of

363 bottom waters in Disko Bugt. This is highlighted by a pronounced peak in cold water
364 species *C. arctica*, *S. biformis* and *R. turbinatus* and *E. excavatum* f. *clavata* (Figs. 5
365 and 6a, b, c). Additionally, we note the reduced abundance of organic detritus
366 feeder's *N. labradorica* and *G. auriculata arctica* (Figs. 3 and 5) suggesting that
367 environmental conditions became harsher compared to the previous interval. We
368 interpret this as a result of a relatively colder WGC reaching Disko Bugt, as a
369 consequence of an increased EGC contribution to the WGC. During this interval, the
370 abundance of sea-ice diatoms from site DA00-03 increases significantly, indicating
371 colder surface waters in Disko Bugt (Fig. 6d; Moros et al. 2006b). The pronounced
372 cooling inferred from benthic foraminifer at c. 2.5 ka BP (Fig. 6b) is possibly related to
373 the 2.8-2.7 ka BP cooling event, given the ΔR uncertainty in the age-depth model (see
374 section 4.1). This cold event is widely reported from marine and terrestrial records
375 over the North Atlantic region (e.g. Oppo et al., 2003; Risebrobakken et al., 2003;
376 Hall et al., 2004; Moros et al., 2004). At about this time, there is evidence of relatively
377 colder temperatures over the Greenland ice sheet, and additionally a cold and
378 relatively fresher EGC from the East Greenland shelf as well as reduced influence of
379 the IC off North Iceland is found (Alley et al., 1999, see Fig. 6e; Andrews et al., 2001;
380 Jennings et al., 2002).

381 A shift towards relatively warmer bottom water conditions off West Greenland
382 is documented from 1.9 to 1.7 ka BP. We find highest abundance of AtIWcalc species
383 at c. 1.8 ka BP, implying a warm phase (see Fig. 6c), which possibly corresponds to
384 the 'Roman Warm Period' and documents the overall 'warmest' bottom water
385 conditions during the last 3.6 ka BP. The predominant calcareous fauna and
386 minimum percentages of AW species *C. arctica*, *S. biformis* and *E. excavatum* f.
387 *clavata* during the RWP (Figs. 4 and 5) documents reduced contribution of the EGC
388 to the WGC at this time in Disko Bugt. A warm phase between 2.2 to 1.4 ka BP in

389 bottom and surface waters (reduced abundance of sea-ice diatoms, see Fig. 6d,
390 Moros et al., 2006b) is also reported from site DA00-03 (Lloyd et al., 2007). In
391 addition, reconstructed temperatures from GISP2 indicate relatively warm
392 atmospheric conditions over the Greenland ice sheet at this time (Alley et al., 1999).
393 This is supported by findings from Jennings et al. (2002), who report a warming
394 within the EGC on the East Greenland shelf from c. 2.1 to 1.4 ka BP, promoted by
395 increased advection of intermediate Atlantic water, which is possibly linked to a
396 strong flow of the NAC.

397 From c. 1.7 ka BP onwards a gradual cooling with decreasing influence of
398 NAC/IC and enhanced advection of EGC waters into the WGC is demonstrated by a
399 progressive rise in abundance of AW species (e.g. *E. excavatum* f. *clavata*, *C. arctica*
400 and *S. biformis*, see Fig. 3 Zone-C). A notable decrease in AtIWcalc species is seen
401 at c. 1.5 ka BP, which coincides remarkably well with a pronounced drop in
402 reconstructed air temperatures from GISP2 ice core (Alley et al., 1999, Fig. 6c,e).
403 These colder conditions in bottom waters lasted only a few decades and possibly
404 correspond to the time period of the Dark Ages.

405 At the transition from the Dark Ages to the time period of the 'Medieval Climate
406 Anomaly' (MCA) we observe only a slight warming in bottom waters in Disko Bugt
407 (rise in AtIWcalc indicators, Fig. 6), as found in studies off East Greenland (Jennings
408 and Weiner, 1996) and the North Iceland shelf (Eiríksson et al., 2006). Compared to
409 the preceding warm phase, the RWP, benthic foraminifera record relatively colder
410 bottom waters during the MCA. This coincides with a pronounced decrease in mean-
411 annual air temperatures recorded in the GISP2 ice core (Alley et al. 1999, Fig. 6e). In
412 support, diatom and dinoflagellate cysts studies from nearby coring sites in Disko
413 Bugt (DA00-02 and DA00-03) identified surface water cooling at about the same time
414 interval (Moros et al., 2006b, see Fig. 6d; Seidenkrantz et al., 2008; Krawczyk et al.,

415 2010). From c. 0.9 ka BP to the present we find a predominant agglutinated fauna
416 established, which indicates a distinct reduction in the contribution of Atlantic water
417 masses (NAC/IC) to the WGC during the LIA. Simultaneously, a decrease in Atlantic
418 water influence on surface-water masses in Disko Bugt is also documented from 0.9
419 ka BP at sites DA00-02 and DA00-03 (Moros et al., 2006b; Lloyd et al., 2007;
420 Seidenkrantz et al., 2008). An ecological threshold was exceeded at 0.7 ka BP. The
421 sudden fall in abundance of *I. norcrossi*, *C. reniforme* and *E. excavatum* f. *clavata*
422 (Fig. 3 and 5, Zone D) and high abundance of AWagg species *C. arctica* and *S.*
423 *biformis*, confirming that environmental conditions became much harsher during this
424 interval. Thus, bottom water temperatures (and possibly salinity) must have dropped
425 to a critical point and chilled AtlW species such as *I. norcrossi* and *C. reniforme* were
426 not able to compete anymore. The disappearance of *E. excavatum* f. *clavata* and
427 other species (e.g. *I. norcrossi* and *C. reniforme*) at the same time as *S. feylingi*
428 increases significantly, supports the interpretation of coldest and harshest conditions
429 in bottom waters from 0.7 ka BP. The peak in *S. feylingi* might also indicate poor
430 ventilation of the water column and depleted/low oxygen content. We believe that *S.*
431 *feylingi* replaces *E. excavatum* f. *clavata* as a consequence of these extreme
432 environmental conditions, supported by highest abundances of agglutinated species.
433 During this time the EGC influence appears strongest on the bottom water mass
434 composition of the WGC is at its strongest over the last 3.6 ka BP (see Fig. 5 and
435 6b). This interval also coincides with coldest temperatures reconstructed from the
436 GISP2 ice core and reconstructed arctic summer temperatures (Alley et al., 1999;
437 Kaufman et al., 2009, see Fig. 6e,f). There is also evidence of a prolonged drift ice
438 pulse off East Greenland during the time of the LIA (Jennings et al., 2002, Moros et
439 al., 2006a) and several authors document glacial advance around Greenland at the
440 same time (e.g. Weidick, 1968; Weidick et al., 1990; Geirsdóttir et al., 2000).

441 Reconstructions from terrestrial archives by Kaufman et al. (2009) document a strong
442 increase in arctic summer temperature during the last c. 100 years. A comparable
443 trend is not observed in subsurface waters in Disko Bugt.

444

445 **5.3 Regional climatic implications**

446 The distinct variability in subsurface water mass properties in Disko Bugt point
447 to broader scale changes in ocean circulation patterns in the source regions of the
448 WGC (e.g. variability in the water mass contribution of the NAC/IC and the EGC).
449 The strong influence of the EGC we document during the late Holocene might be
450 linked to enhanced outflow of arctic water masses into the polar North Atlantic. This
451 is supported by evidence of increased drift ice occurrence (Andrews et al., 1997;
452 Jennings et al., 2002; Moros et al., 2006a) and increased IRD deposition in the
453 Denmark Strait (Jennings et al., 2011). Increased advection of fresher Arctic-derived
454 waters into the northern North Atlantic by the EGC can lead to reduced deep-water
455 formation in the Labrador and Nordic Seas and can consequently cause a weakening
456 of the Subpolar Gyre (SPG). Weakening of the SPG may in turn have a strong impact
457 on the flow of the NAC and Atlantic Meridional Overturning Circulation (Hillaire-
458 Marcel et al., 2001; Häkkinen and Rhines, 2004; Hátún et al., 2005). However,
459 Thornalley et al. (2009) discuss a relatively reduced and more fluctuating SPG
460 activity during the late Holocene and suggest a weakened SPG circulation is likely to
461 be linked to atmospheric circulation, i.e. decreased wind stress rather than enhanced
462 freshwater flux from the Arctic. This would allow a stronger EGC influx to the WGC.
463 Studies from eastern Canada (Kasper and Allard, 2001) and south Greenland
464 (Lassen et al., 2004; Kuijpers and Mikkelsen, 2009; Jessen et al., in press), relate
465 changes in atmospheric circulation patterns to a shift from a predominant NAO⁺ to a
466 NAO⁻ regime over this time period. Intervals of relative increase in the influence of the

467 warm NAC/IC on the WGC 3.6 to 2.6 ka BP and at c. 1.8 ka BP, may imply a more
468 NAO⁺ regime, while intervals of stronger EGC influence 2.6 to 1.9 ka BP and from 0.9
469 ka BP onwards, possibly reflect a more NAO⁻ like regime in West Greenland.

470

471

472 **6. Summary and conclusions**

473 Our new high-resolution benthic foraminiferal study from Egedesminde Dyb
474 provides a long-term record at decadal resolution of variations in subsurface water
475 mass (WGC) composition off West Greenland during the late Holocene (since 3.6 ka
476 BP). A longer-term cooling trend is observed, which becomes most pronounced from
477 c. 1.7 ka BP onwards, as calcareous Atlantic water species decrease significantly
478 and agglutinated Arctic water species increase. This cooling trend reflects increasing
479 EGC influence on the WGC which can be either attributed to increasing meltwater
480 and drift ice input in the EGC source region or to changes in the atmospheric North
481 Atlantic Oscillation system from a NAO⁺ to a predominant NAO⁻ regime over the late
482 Holocene. This longer-term late Holocene cooling trend in the basal waters of Disko
483 Bugt culminates with the Little Ice Age at 0.3 ka BP.

484 Our findings support previous studies from Disko Bugt and adjacent West
485 Greenland fjords, which reported a gradual cooling of subsurface waters since the
486 Holocene Thermal Maximum at c. 6 to 5 ka BP. Superimposed on this longer-term
487 late Holocene cooling trend, we document millennial to centennial scale variability. A
488 pronounced cooling event is found at c. 2.5 ka BP (corresponding to the 2.7 - 2.8 ka
489 BP cooling event), which is also recorded in marine and terrestrial archives
490 elsewhere in the North Atlantic region. A warm phase in bottom waters is recorded at
491 c. 1.8 ka BP, which corresponds to the 'Roman Warm Period' and is seen to
492 represent the warmest bottom water conditions recorded in Disko Bugt during the last

493 3.6 ka BP. However, only a slight warming is observed in subsurface waters during
494 the 'Medieval Climate Anomaly'. From 0.9 ka BP we find pervasive and even harsher
495 environmental conditions (e.g. limited food availability), highlighted by the sudden fall
496 in abundance of *Cassidulina reniforme*, *Islandiella norcrossi* and *Elphidium*
497 *excavatum* f. *clavata* as an ecological threshold is exceeded. Peak abundance of
498 *Stainforthia feylingi* and agglutinated Arctic water species (e.g. *Cuneata arctica* and
499 *Spiroplectammina biformis*) reflect the culmination of this cooling trend at 0.3 ka BP
500 (Little Ice Age). Reconstructions from arctic terrestrial archives match, to some extent
501 the late Holocene longer-term cooling trend in the basal waters in Disko Bugt. The
502 reconstructed increased influence of the EGC on bottom waters in Disko Bugt may
503 also have a strong influence on the flow of the North Atlantic Current.

504

505

506 **Acknowledgements**

507 The authors thank the Deutsche Forschungsgemeinschaft (DFG) for funding the
508 project 'Disko Climate' (MO 1422/2-1). Further we thank Captain and Crew of the R/V
509 'Maria S. Merian' for their fantastic work during cruise MSM05/03. We also thank
510 Anne Jennings, Karen Luise Knudsen and Marit Solveig Seidenkrantz for fruitful
511 discussion of the benthic foraminiferal assemblage and their interpretation. We thank
512 Bernd Wagner and Volker Wennrich for producing X-radiographs of the sediment
513 core at the University of Cologne and Tomasz Goslar from Poznań Radiocarbon
514 Laboratory. The constructive comments of 2 anonymous reviewers also helped to
515 improve the manuscript.

516

517

518

519

520

521 **References**

522 **Alley, R.B., Agustsdottir, A.M., and Fawcett, P.J.**, 1999. Ice-core evidence of late-
523 Holocene reduction in North Atlantic Ocean heat transport. *Geophysical*
524 *Monograph* 112, 301–312.

525 **Alve, E.**, 1990. Variations in estuarine foraminiferal biofacies with diminishing
526 oxygen conditions in Drammensfjord. SE Norway. *In*: Hemleben, C., Kaminski,
527 M. A., Kuhnt, W., and Scott, D. B. (eds.), *Paleoecology, Biostratigraphy,*
528 *Paleoceanography and Taxonomy of Agglutinated Foraminifera: NATO AS1*
529 *Series., Series C, Mathematical and Physical Sciences, Kluwer Academic*
530 *Publishers, Dordrecht*, 327, 661-694.

531 **Alve, E.**, 1994. Opportunistic features of the foraminifer *Stainforthia fusiformis*
532 (Williamson): evidence from Frierfjord, Norway. *Journal of Micropalaeontology*
533 13, 24.

534 **Andersen, C., Koç, N., Jennings, A.E., and Andrews, J.T.**, 2004. Nonuniform
535 response of the major surface currents in the Nordic Seas to insolation
536 forcing: implications for the Holocene climate variability. *Paleoceanography*
537 19, PA2003.

538 **Anderson, L., Abbott, M.B., Finney, B.P., and Burns, S.J.**, 2006. Regional
539 atmospheric circulation change in the North Pacific during the Holocene
540 inferred from lacustrine carbonate oxygen isotopes, Yukon Territory, Canada.
541 *Quaternary Research* 65, 350-351.

542 **Andersson, C., Risebrobakken, B., Jansen, E., and Dahl, S.O.**, 2003. Late
543 Holocene surface ocean conditions of the Norwegian Sea (Vöhring Plateau).
544 *Paleoceanography* 18, PA1044.

545 **Andresen, O.G.N.**, 1981. The annual cycle of temperature, salinity, currents and
546 water masses in Disko Bugt and adjacent waters, West Greenland.
547 Meddelelser om Grønland, Bioscience 5, 1-36.

548 **Andrews, J. T., Smith, L. M., Preston, R., Cooper, T., and Jennings, A. E.**, 1997.
549 Spatial and temporal patterns of iceberg rafting (IRD) along the east
550 Greenland margin, ca.68 N, over the last 14 cal. ka. J. Quat. Sci. 12,
551 1 –13.

552 **Andrews, J. T., Caseldine, C., Weiner, N. J., and Hatton, J.**, 2001. Late
553 Quaternary (~4 ka) marine and terrestrial environmental change in
554 Reykjarfjörður, N. Iceland: Climate and/or settlement? J. Quat. Sci. 16, 133–
555 144.

556 **Bâcle, J.E., Carmack, C., and Ingram, R.G.**, 2002. Water column structure and
557 circulation in the North Water during spring transition: April-July 1998, Deep
558 Sea Research 49, 4907 – 4925.

559 **Bernhard, J. M., and Alve, E.**, 1996. Survival, ATP pool, and ultrastructural
560 characterization of benthic foraminifera from Drammensfjord (Norway):
561 response to anoxia. Marine Micropaleontology 28, 5–17.

562 **Bronk Ramsey, C.**, 2009. Bayesian analysis of radiocarbon dates. Radiocarbon 51,
563 pp. 337.

564 **Buch, E.**, 1981. A Review of the oceanographic conditions in subarea O and 1 in the
565 decade 1970- 79. NAFO Symposium on Environmental conditions in the
566 Northwest Atlantic during 1970-79. NAFO Scientific Council Studies no.5.

567 **Buch, E., Pedersen, S.A., and Ribergaard, M.H.**, 2004. Ecosystem Variability in
568 West Greenland Waters. Journal of Northw. Atl. Fish. Sci. 34, 13-28.

569 **Corliss, B.H.**, 1991. Morphology and microhabitat preferences of benthic

570 foraminifera from the northwest Atlantic Ocean. *Marine Micropaleontology* 17,
571 195-236.

572 **Corliss, B.H. and Chen, C.**, 1988. Morphotype patterns of Norwegian Sea deep-sea
573 benthic foraminifera and ecological implications. *Geology* 16, 716-719.

574 **Dahl-Jensen, D., Mosegaard, K., Gundestrup, N., Clow, G.D., Johnsen, S.J.,**
575 **Hansen, A.W., and Balling, N.**, 1998. Past temperature directly from the
576 greenland ice sheet. *Science* 282, 268–271.

577 **de Vernal, A., and Hillaire-Marcel, C.**, 2006. Provincialism in trends and high
578 frequency changes in the northwest North Atlantic during the Holocene. *Global*
579 *and Planetary Change* 54, 263-390.

580 **Duplessy, J-C., Invanova, E.V., Murdmaa, I.O, Paterne, M., and Labyrie, L.**, 2001.
581 Holocene palaeoceanography of the northern Barents Sea and variations of the
582 northward heat transport by the Atlantic Ocean. *Boreas*, 30(1), 2-16.

583 **Elverhøi, A., Liestøl, O., and Nagy, J.**, 1980. Glacial erosion, sedimentation
584 and microfauna in the inner part of Kongsfjord, Spitsbergen:
585 *Norsk Polarinstitutt Skrifter*, 172, 33–61.

586 **Feyling-Hansen, R., and Funder, S.**, 1990. Fauna and flora. In: S. Funder (Editor),
587 Late Quaternary Stratigraphy and Glaciology in the Thule area. *Medd. Gronl.*
588 *Geosci.*, 22, 19-33.

589 **Fréchette, B. and de Vernal, A.**, 2009. Relationship between Holocene climate
590 variations over southern Greenland and eastern Baffin Island and synoptic
591 circulation pattern. *Climate of the Past* 5, 247-359.

592 **Funder, S. and Weidick, A.**, 1991. Holocene boreal molluscs in Greenland –
593 palaeoceanographic implications. *Palaeogeography, Palaeoclimatology,*
594 *Palaeoecology* 85, 123–35.

595 **Geirsdóttir, A., Hardardóttir, J. and Andrews, J.T.**, 2000. Late-Holocene terrestrial

596 glacial history of Miki and I.C. Jacobsen Fjords, East Greenland. The Holocene
597 10, 123–34.

598 **Giraudeau, J., Jennings, A.E., and Andrews, J.T.**, 2004. Timing and mechanisms
599 of surface and intermediate water circulation changes in the Nordic Seas over
600 the last 10 000 cal. Years: a view from the North Iceland shelf. Quaternary
601 Science Reviews 23, 2127-2139.

602 **Hald, M., and Steinsund, P.I.**, 1992. Distribution of surface sediment benthic
603 foraminifera in the southwestern Barents Sea. Journal of Foraminiferal
604 Research 21, 347–62.

605 **Hald, M., Dokken, T., Korsun, S., Polyak, L., and Aspeli, R.**, 1994. Recent and
606 Late Quaternary distribution of *Elphidium excavatum* f. *clavata* in Arctic seas:
607 Cushman Foundation Special Publication 32, 141–153.

608 **Hald, M. and Steinsund, P.I.**, 1996. Benthic foraminifera and carbonate dissolution
609 in surface sediments of the Barents- and Kara Seas. Ber. Polarforsch., 21 2 (1
610 996).

611 **Hald, M. and Korsun, S.**, 1997. Distribution of modern benthic foraminifera from
612 fjords of Svalbard, European Arctic. Journal of Foraminiferal Research 27,
613 101–22.

614 **Hall, I.G., Bianchi, G., and Evans, J.R.**, 2004. Centennial to millennial scale
615 Holocene climate-deep water linkages in the North Atlantic. Quaternary
616 Science. Reviews 23, 1529– 1536.

617 **Hansen, A., and Knudsen, K.L.**, 1995. Recent foraminiferal distribution in
618 Freemansundet and Early Holocene stratigraphy on Edgeøya, Svalbard:
619 Polar Research 14, 215–238.

620 **Harff, J., Dietrich, R., Endler, R., Hentzsch, B., Jensen, J. B., Kuijpers, A.,**
621 **Krauss, N., Leipe, Th., Lloyd, J., Mikkelsen, N., Moros, M., Perner, K.**

622 **Richter, A., Risgaard-Petersen, N., Rysgaard, S., Richter, Th.,**
623 **Sandgren, P., Sheshenko, V., Snowball, I., Waniek, J., Weinrebe, W., and**
624 **Witkowski, A., 2007.** Deglaciation history, coastal development, and
625 environmental change during the Holocene in western Greenland. Cruise
626 report R/V Maria S. Merian, cruise MSM 05/03.

627 **Häkkinen, S. and Rhines, P. B., 2004.** Decline of subpolar North Atlantic circulation
628 during the 1990s. *Science* 304, 555–559.

629 **Hátún, H., Sando, A.B., Drange, H., Hansen, B. and Valdimarsson, H., 2005.**
630 Influence of the Atlantic subpolar gyre on the thermohaline circulation. *Science*
631 309, 1841–1844.

632 **Heegaard, E., Birks, H.J.B., Telford, J.T., 2005.** Relationships between calibrated
633 ages and depth in stratigraphical sequences: an estimation procedure by
634 mixedeffect regression. *The Holocene* 15, 612–618.

635 **Hillaire-Marcel, C., de Vernal, A., Bilodeau, G. and Weaver, A., 2001.** Absence of
636 Deepwater formation in the Labrador Sea during the last interglacial period.
637 *Nature* 410, 1073–1077.

638 **Holland, D.M., Thomas, R.H., De Young, B., Ribergaard, M.H., and Lyberth, B.,**
639 2008. Acceleration of Jakobshavn Isbrae triggered by warm subsurface ocean
640 waters. *Nature Geoscience* 1, 659.

641 **Humlum, O., 1999.** Late Holocene Climate in Central West Greenland:
642 Meteorological Data and Rock Glacier Isotope Evidence. *The Holocene* 9 (5),
643 581-594.

644 **Jennings, A.E., and Helgadottir, G., 1994.** Foraminiferal assemblages from the
645 fjords and shelf of eastern Greenland. *Journal of Foraminiferal Research* 24,
646 123–44.

647 **Jennings, A., and Weiner, N., 1996.** Environmental change in eastern Greenland

648 during the last 1300 years: evidence from foraminifera and lithofacies in
649 Nansen Fjord, 68°N. *The Holocene* 6, 179–91.

650 **Jennings, A.E., Hagen, S., Hardardottir, J., Stein, R., Ogilvie, A.E.J.**
651 **and Jonsdottir, I.**, 2001. Oceanographic change and terrestrial human
652 impacts in a post A.D. 1400 sediment record from the southwest Iceland
653 shelf. *Climatic Change* 48 (Special Issue, The Iceberg in the Mist: Northern
654 Research in Pursuit of 'A Little Ice Age', guest editors Ogilvie, A.E.
655 and Jónsson, T.), 83–100.

656 **Jennings, A., Knudsen, K.L., Hald, M., Hansen, C.V. and Andrews, J.T.**, 2002. A
657 mid-Holocene shift in Arctic sea-ice variability on the East Greenland Shelf.
658 *The Holocene* 12, 49–58.

659 **Jennings, A., Weiner, N.J., Helgadottir, G. and Andrews, J.T.**, 2004. Modern
660 foraminiferal faunas of the southwestern to northern Iceland shelf:
661 oceanographic and environmental controls. *Journal of Foraminiferal Research*
662 34, 180–207.

663 **Jennings, A., Andrews, J., Wilson, L.**, 2011. Holocene environmental evolution of
664 the SE Greenland Shelf North and South of the Denmark Strait: Irminger and
665 East Greenland current interactions. *Quaternary Science Reviews* 30, 980-
666 998.

667 **Jessen, C., Solignac, S., Nørgaard-Pedersen, N., Kuijpers, A., and Seidenkrantz,**
668 **M.S.**, 2011. Exotic pollen as an indicator of variable atmospheric circulation
669 over the Labrador Sea region during the mid to late Holocene. *Journal of*
670 *Quaternary Science* 26, 286-296.

671 **Jorissen, F.J., de Stigter, H.C., and Widmark, J.G.V.**, 1995. A conceptual model
672 explaining benthic foraminiferal microhabitats. *Marine Micropaleontology* 26, 3-
673 15.

674 **Kalish, J.M., Nydal, R., Nedreaas, K.H., Burr, G.S., and Eine, G.L.,** 2001. A time
675 history of pre- and post-bomb radiocarbon in the Barents Sea derived from
676 Arcto-Norwegian cod otoliths. *Radiocarbon* 43, 843.

677 **Kaufman, D.S., Ager, T.A., Anderson, N.J., Anderson, P.M., Andrews, J.T.,**
678 **Bartlein, P.J., Brubaker, L.B., Coats, L.L., Cwynar, L.C., Duvall, M.L.,**
679 **Dyke, A.S., Edwards, M.E., Eisner, W.R., Gajewski, K., Geirsdóttir, A., Hu,**
680 **F.S., Jennings, A.E., Kaplan, M.R., Kerwin, M.W., Lozhkin, A.V.,**
681 **MacDonald, G.M., Miller, G.H., Mock, C.J., Oswald, W.W., Otto-Bliesner,**
682 **B.L., Porinchu, D.F., Rühland, K., Smol, J.P., Steig, E.J. and Wolfe, B.B.,**
683 2004. Holocene thermal maximum in the western Arctic (0–180°W).
684 *Quaternary Science Reviews* 23, 529–60.

685 **Kaufman, D.S., Schneider, D.P., McKay, N.P., Ammann, C.A., Bradley, R.S.,**
686 **Briffa, K.R., Miller, G.H., Otto-Bliesner, B.L., Overpeck, J.T., Vinther, B.M.,**
687 **and Arctic Lakes 2k Project Members,** 2009. Recent warming reverses long-
688 term Arctic cooling. *Science* 325, 1236.

689 **Kasper, J.N., and Allard, M.,** 2001. Late Holocene climatic changes as detected by
690 the growth and decay of ice wedges on the southern shore of Hudson Strait,
691 northern Quebec, Canada. *The Holocene* 11, 563–577.

692 **Kelly, M.,** 1979. Comments on the implications of new radiocarbon dates from the
693 Holsteinsborg region, central West Greenland. *Gronl. Geol. Unders. Rep.*, 95,
694 35-42.

695 **Kelly, M.,** 1980. The status of the Neoglacial in western Greenland. *Rapport*
696 *Grønlands Geologiske Undersøgelse* 96, 1–24.

697 **Kelly, M.,** 1985. A review of the Quaternary geology of western Greenland. In: J. T.
698 Andrews (Editor), *Quaternary Environments eastern Canadian Arctic, Baffin*
699 *Bay and western Greenland.* Allen and Unwin, Boston, pp. 461-501.

700 **Knudsen, K.L., and Seidenkrantz, M.-S.** 1994. *Stainforthia feylingi* new species
701 from arctic to subarctic environments, previously recorded as *Stainforthia*
702 *schreibersiana* (Czjzek). Cushman Foundation for Foraminiferal Research
703 Special Publication, 32:5-13.

704 **Knudsen, K.L., Eiríksson, J., Jansen, J., Jiang, H., Rytter, F., and**
705 **Gudmundsdóttir, E.R.,** 2004. Palaeoceanographic changes off North Iceland
706 through the last 1200 years: foraminifera, stable isotopes, diatoms and ice
707 rafted debris. *Quaternary Science Reviews* 23, 2231–2246.

708 **Korsun, S., and Hald, M.,** 1998. Modern benthic foraminifera off Novaya Zemlya
709 tidewater glaciers, Russian Arctic. *Arctic and Alpine Research* 30, 61–77.

710 **Krawczyk, D., Witkowski, A., Moros, M., Lloyd, J.M., Kuijpers, A. and Kierzek, A.**
711 2010. Late-Holocene diatom-inferred reconstruction of temperature variations
712 of the West Greenland Current from Disko Bugt, central West Greenland. *The*
713 *Holocene* 20 (5), 659-666.

714 **Krog, H. and Tauber, H.,** 1974. C-14 chronology of Late and Postglacial marine
715 deposits in North Jutland, *Danmarks Geologiske Undersøgelse Årbog* 1973,
716 93–105.

717 **Kuijpers, A. and Mikkelsen, N.,** 2009. Geological records of changes in wind regime
718 over south Greenland since the Medieval Warm Period: a tentative
719 reconstruction. *Polar Record* 45 (232),1-8.

720 **Lassen, S.J., Kuijpers, A., Kunzendorf, H., Hoffman-Wieck, G., Mikkelsen, N.**
721 **and Konradi, P.,** 2004. Late-Holocene Atlantic bottom water variability in
722 Igaliku Fjord, South Greenland, reconstructed from foraminifera faunas. *The*
723 *Holocene* 14, 165–171

724 **Lloyd, J.M., Park, L.A., Kuijpers, A. and Moros, M.,** 2005. Early Holocene

725 palaeoceanography and deglacial chronology of Disko Bugt, West Greenland.
726 Quaternary Science Reviews 24, 1741–1755.

727 **Lloyd, J.M.**, 2006a. Late Holocene environmental change in Disko Bugt, west
728 Greenland: interaction between climate, ocean circulation and Jakobshavn
729 Isbrae. *Boreas* 35, 36–49.

730 ——— 2006b. Modern distribution of benthic foraminifera from Disko Bugt, west
731 Greenland. *Journal of Foraminiferal Research* 36, 315–331.

732 **Lloyd, J.M., Kuijpers, A., Long, A., Moros, M., and Park, L.A.**, 2007. Foraminiferal
733 reconstruction of mid- to late-Holocene ocean circulation and climate variability
734 in Disko Bugt, West Greenland. *The Holocene* 17, 1079-1091.

735 **Lloyd, J.M., Moros, M., Perner, K., Telford, R., Kuijpers, A., Jansen, E., and**
736 **McCarthy, D.J.**, 2011. A 100 year record of ocean temperature control on the
737 stability of Jakobshavn Isbrae, West Greenland. *Geology* (in press).

738 **Mackensen, A., Sejrup, H.P., and Jansen, E.**, 1985. The distribution of living
739 benthic foraminifera on the continental slope and rise off southwest Norway.
740 *Marine Micropaleontology* 9, 275–306.

741 **Madsen, H.B. and Knudsen, K.L.**, 1994. Recent foraminifera in shelf sediments of
742 the Scoresby Sund fjord, East Greenland. *Boreas* 23, 495–504.

743 **McNeely, R., Dyke, A.S, and Southon, JR.**, 2006. Canadian marine reservoir ages,
744 preliminary data assessment. Open File 5049. Geological Survey of Canada,
745 pp.3.

746 **Møller, H.S., Jensen, K.G., Kuijpers, A., Aagaard-Sørensen, S., Seidenkrantz,**
747 **M.-S., Prins, M., Endler, R. and Mikkelsen, N.**, 2006. Late-Holocene
748 environment and climatic changes in Ameralik fjord, southwest Greenland:
749 evidence from the sedimentary record. *The Holocene* 16, 685–695.

750 **Moros, M., Emeis, K., Risebrobakken, B., Snowball, I., Kuijpers, A., McManus,**

751 **J. and Jansen, E.**, 2004. Sea surface temperatures and ice rafting in the
752 Holocene North Atlantic: climate influences on northern Europe and
753 Greenland. *Quaternary Science Reviews* 23, 2113–2126.

754 **Moros, M., Andrews, J.T., Eberl, D.D. and Jansen, E.**, 2006a. Holocene history of
755 drift ice in the northern North Atlantic: Evidence for different spatial and
756 temporal modes. *Paleoceanography* 21, 2017.

757 **Moros, M., Jensen, K.G. and Kuijpers, A.**, 2006b. Mid- to late- Holocene
758 hydrological and climatic variability in Disko Bugt, central West Greenland. *The*
759 *Holocene* 16, 357–367.

760 **Mudie, P.J., Keen, C.E., Hardy, I.E. and Vilks, G.**, 1984. Multivariate analysis and
761 quantitative paleoecology of benthic foraminifera in surface and Late
762 Quaternary shelf sediments, northern Canada. *Marine Micropalaeontology* 8,
763 283–313.

764 **Mudie, P.J., Rochon, A. and Levac, E.**, 2005. Decadal-scale sea ice changes in the
765 Canadian Arctic and their impacts on humans during the past 4,000 years.
766 *Environmental Archaeology* 10, 113–126.

767 **Murray, J.W.**, 1991. *Ecology and palaeoecology of benthic foraminifera*. Longman,
768 London, 397pp.

769 **Nagy, J.**, 1965. Foraminifera in some bottom samples from shallow
770 waters in Vestspitsbergen: *Norks Polarinstitut Arbok* 1963, p. 109–125.

771 **Oppo, D.W., McManus, J.F., and Cullen, J.R.**, 2003. Palaeoceanography:
772 deepwater variability in the Holocene epoch. *Nature* 422, 277.

773 **Osterman, L.E. and Nelson, A.R.**, 1989. Latest Quaternary and Holocene
774 paleoceanography of the eastern Baffin Island continental shelf, Canada:
775 benthic foraminiferal evidence. *Canadian Journal of Earth Science* 26, 2236–
776 2248.

- 777 **Ólafsdóttir, S., Jennings, A. E., Geisdóttir, Á., Andrews, J., and Miller, G., 2010.**
778 Holocene variability of the North Atlantic Irminger current on the south- and
779 northwest shelf of Iceland. *Marine Micropaleontology* 77 (3-4), 101-118.
- 780 **Polyak, L. and Solheim, A., 1994.** Late- and postglacial environments in the
781 northern Barents Sea west of Franz Josef Land. *Polar Research* 13, 197–207.
- 782 **Ran, L., Jiang, H., Knudsen, K.L., and Eiríksson, J., 2008.** The mid- to late
783 Holocene paleoceanographic changes in the northern North Atlantic. *Front.*
784 *Earth Sci. China*, 1(4), 449-457.
- 785 **Rasmussen, T.L., Thomsen, E., Troelstra, S.R., Kuijpers, A., and Prins, M.A.,**
786 2002. Millennial-scale glacial variability versus Holocene stability: changes in
787 planktic and benthic foraminifera faunas and ocean circulation in the North
788 Atlantic during the last 60 000 years. *Marine Micropaleontology*, 47, 143-176.
- 789 **Reimer, P.J., and Reimer, R.W., 2001.** A marine reservoir correction database and
790 on-line interface. *Radiocarbon* 43, 46.
- 791 **Reimer, P.J., Baillie, M.G.L., Bard, E., Bayliss, A., Beck, J.W., Blackwell, P.G.,**
792 **Bronk Ramsey, C., Buck, C.E., Burr, G.S, Edwards, R.L., Friedrich, M.,**
793 **Grootes, P.M., Guilderson, T.P., Hajdas, I., Heaton, T.J., Hogg, A.G.,**
794 **Hughen, K.A., Kaiser, K.F., Kromer, B., McCormac, F.G., Manning, S.W.,**
795 **Reimer, R.W., Richards, D.A., Southon, J.R., Talamo, S., Turney, C.S.M,**
796 **van der Plicht, J., and Weyhenmeyer, C.E., 2009.** IntCal09 and Marine09
797 radiocarbon age calibration curves, 0-50,000 years cal BP. *Radiocarbon* **51**,
798 1111-1150.
- 799 **Rignot, E., Koppes, M., and Velicogna, I., 2010.** Rapid submarine melting of the
800 calving faces of West Greenland glaciers. *Nature Geoscience* 3, 187.
- 801 **Risebrobakken, B., Jansen, E., Andersson, C., Mjelde, E., and Hevroy, K., 2003.**

802 A high-resolution study of Holocene paleoclimatic and paleoceanographic
803 changes in the Nordic Seas. *Paleoceanography* 18, 1017–1031.

804 **Rytter, F., Knudsen, K.L., Seidenkrantz, S. and Eiriksson, J.**, 2002. Modern
805 distribution of benthic foraminifera on the North Icelandic shelf and slope.
806 *Journal of Foraminiferal Research* 32, 217–244.

807 **Schafer, C.T and Cole, F.E.**, 1986. Reconnaissance survey of benthonic
808 foraminifera from Baffin Fjord environments. *Arctic* 39, 232–239.

809 **Schröder-Adams, C.J., Mudie, P.J., Cole, F.E., and Medioli, F.S.**, 1990. Late
810 Holocene Benthic Foraminifera beneath Perennial Sea Ice on an Arctic
811 Continental Shelf. *Marine Geology* 93, 225-242.

812 **Seidenkrantz, M.-S., Aagaard-Sørensen, S., Sulsbrück, S., Kuijpers, A., Jansen,**
813 **K.G. and Kunzendorf, H.**, 2007. Hydrography and climate of the last 4400
814 years in a SW Greenland fjord – implications for Labrador Sea
815 palaeoceanography. *The Holocene* 17, 387–401.

816 **Seidenkrantz, M.-S., Roncaglia, L., Fischel, A., Heilmann-Clausen, C., Kuijpers,**
817 **A., and Moros, M.**, 2008. Variable North Atlantic seesaw patterns
818 documented by a late Holocene marine record from Disko Bugt, West
819 Greenland. *Marine Micropaleontology* 68, 66-83.

820 **Sejrup, H.P., Birks, H.J.B., Klitgaard-Kristensen, D., Madsen, H.**, 2004. Benthonic
821 foraminiferal distributions and quantitative transfer functions for the northwest
822 European continental margin. *Marine Micropaleontology* 53, 197-226.

823 **Steinsund, P.I., Polyak, L., Hald, M., Mikhailov, V. and Korsun, S.**, 1994.
824 Distribution of calcareous benthic foraminifera in recent sediments of the
825 Barents and Kara Sea. In Steinsund, P.I., *Benthic foraminifera in surface*
826 *sediments of the Barents and Kara Seas: modern and late Quaternary*

827 application. Ph.D. thesis, Department of Geology, Institute of Biology and
828 Geology, Univeristy of Tromsø.

829 **Tauber, H. and Funder, S.**, 1975. ^{14}C content of recent molluscs from Scoresby
830 Sund, central East Greenland. Gronlands Geologiske Undersogelse, Rapport
831 75, 95–99.

832 **Tauber, H.**, 1979. ^{14}C activity of arctic marine mammals. In: R. Berger and H.E.
833 Suess, Editors, *Radiocarbon Dating*, University of California Press, 447–452.

834 **Thornalley, D.J.R., Elderfield, H., and McCave, I.N.**, 2009. Holocene oscillations in
835 temperature and salinity of the surface subpolar North Atlantic. *Nature*, 457 (5)
836 711-714.

837 **Vilks, G., and Rashid, M.A.**, 1976. Post-glacial paleo-oceanography of Emerald
838 Basin, Scotian Shelf. *Canadian Journal of Earth Sciences* 9, 1256-1267.

839 **Vilks, G.**, 1981. Late glacial–postglacial foraminiferal boundary in sediments
840 of eastern Canada, Denmark and Norway. *Geoscience Canadian* 8, 48–56.

841 **Vilks, G.**, 1989. Ecology of Recent foraminifera on the Canadian continental
842 shelf of the Arctic Ocean, *in* Herman, Y. (ed.), *The Arctic Seas—Climatology,*
843 *Oceanography, Geology and Biology*: Van Nostrand Reinhold, New York, p.
844 497–569.

845 **Vinther, B. M., Buchardt, S. L., Clausen, H. B., Dahl-Jensen, D., Johnsen, S**
846 **. J., Fisher, D. A., Koerner, R. M., Raynaud, D., Lipenkov, V., Andersen, K.**
847 **K., Blunier, T., Rasmussen, S. O., Steffensen, J. P., and Svensson, A.M.**,
848 2009. Holocene thinning of the Greenland ice sheet. *Nature* 461, 385-388.

849 **Weidick, A.**, 1968. Observations on some Hoiocene glacier fluctuations in West
850 Greenland. *Medd. Gronl.*, 165 (6), 202 pp.

851 **Weidick, A., Oerter, H., Reeh, N., Thomsen, H.H. and Thorning, L.**, 1990. The

852 recession of the Inland Ice margin during the Holocene climatic optimum in the
853 Jakobshavn Isfjord area of West Greenland. *Palaeogeography,*
854 *Palaeoclimatology, Palaeoecology* 82, 389–399.

855 **Williamson, M.A., Keen, C.E., and Mudie, P.J.**, 1984. Foraminiferal distribution on
856 the continental margin off Nova Scotia. *Marine Micropaleontology* 9, 219–239.

857 **Wollenburg, J., Knies, J., Machensen, A.**, 2004. High-resolution palaeoproductivity
858 fluctuations 245 during the last 24 kyr indicated by benthic foraminifera in the
859 marginal Arctic Ocean: 246 *Palaeogeography, Palaeoclimatology,*
860 *Palaeoecology* 204, 209-238.

861 **Zarudzki, E.F.K.**, 1980. Interpretation of shallow seismic profiles over the continental
862 shelf in West Greenland between latitudes 64° and 69° 30' N. *Geological*
863 *Survey of Greenland Report* 100, 58-61.

864

865 **Figure captions**

866

867 **Fig.1:** Map of Disko Bugt showing location of core 343310 in south-western
868 Egedesminde Dyb. The insert map shows the present day oceanographic setting of
869 the study area. Abbreviations are as follow: EGC - East Greenland Current; IC –
870 Irminger Current; WGC – West Greenland Current; LC – Labrador Current.

871 **Fig.2:** Age/depth model of 343310 (gravity core). AMS ^{14}C dates are calibrated with
872 the Marine09 (Reimer et al., 2009) calibration curve using OxCal 4.1 (Bronk Ramsey,
873 2009). For AMS ^{14}C dates refer to Table 1.

874 **Fig.3: Combined calcareous and agglutinated foraminiferal assemblage** from
875 site 343310 versus age. Foraminiferal frequencies are expressed as a percentage of
876 the total specimens counted. Only species with an abundance greater than 10% are
877 included. Additionally, the percentage abundance of agglutinated species, total
878 counts and grouping of AtIW (red color) and AW (blue color) indicator species are
879 presented.

880 **Fig.4: Agglutinated foraminiferal assemblage** of site 343310 versus age.
881 Foraminiferal frequencies are expressed as a percentage of total agglutinated
882 specimens counted. Only species with an abundance greater than 5% are included.

883 **Fig.5: Calcareous foraminiferal assemblage** of site 343310. Foraminiferal
884 frequencies are expressed as a percentage of total calcareous specimens counted.
885 Only species with an abundance greater than 5% are included plus selected
886 specimens.

887 **Fig.6:** Summary from 343310 and other regional datasets for comparison. (a) Ratio
888 of calcareous vs. agglutinated specimens; (b) Relative abundance of agglutinated

889 Arctic water species, note the inverse scale; (c) Relative abundance of calcareous
890 chilled Atlantic water species; (d) Relative abundance of sea-ice diatoms from site
891 DA00-03 from Moros et al. (2006b); (e) mean annual temperature reconstructions
892 from GISP2 ice core from Alley et al. (1999); (f) Reconstructed arctic summer
893 temperature from Kaufmann et al. (2009). Known climatic events such as the Roman
894 Warm Period (RWP), The Dark Ages (DA), the Medieval Climate Anomaly (MCA)
895 and the 'Little Ice Age' (LIA) are indicated. Grey arrows indicate 2.7-2.8 ka cooling
896 event.

897

898 Table 1. Radiocarbon dates for gravity core 343310.

depth (cm)	Lab. code	Material	Mass mgC	¹⁴ C date yrs BP (pMC)	Calibrated yrs BP 1950	Years (A.D./B.C.)
6 – 10	Poz-33417	mix benthic forams	NA	671 ± 29 (92 ± 0.4 pMC)	110 – 250	AD 1840 - 1710
18 – 20	Poz-33412	mix benthic forams	NA	659 ± 33 (92.1 ± 0.4 pMC)	90 – 240	AD 1860 - 1710
18 – 19	Poz-22357	Mollusc shell	NA	682 ± 32 (91.8 ± 0.4 pMC)	120 – 260	AD 1830 - 1690
90 – 92	Poz-33453	mix benthic forams	NA	909 ± 35 (89.3 ± 0.4 pMC)	360 – 470	AD 1590 - 1480
149 - 151	Poz-33411	mix benthic forams	NA	1216 ± 30 (86 ± 0.3 pMC)	600 – 680	AD 1350 - 1270
204 - 205	Poz-30969	Mollusc shell	NA	1384 ± 27 (84.2 ± 0.3 pMC)	730 – 840	AD 1220 - 1270
269 - 271	Poz-33413	mix benthic forams	NA	1526 ± 34 (82.7 ± 0.4 pMC)	880 - 990	AD 1070 - 960
340 - 342	Poz-33488	mix benthic forams	NA	1768 ± 46 (80.2 ± 0.5 pMC)	1130 - 1260	AD 820 - 690
400 - 401	Poz-33414	mix benthic forams	NA	2074 ± 29 (77.2 ± 0.3 pMC)	1410 - 1530	AD 540 – 420
401 - 402	Poz-22359	Mollusc shell	NA	2029 ± 28 (77.7 ± 0.3 pMC)	1380 - 1490	AD 570 - 460
457 - 458	Poz-30970	mix benthic forams	NA	2198 ± 31 (76.1 ± 0.3 pMC)	1560 - 1690	AD 390 - 260
519 - 521	Poz-33416	mix benthic forams	NA	2356 ± 35 (74.6 ± 0.3 pMC)	1750 - 1880	AD 200 - 70
600 - 601	Poz-30971	Mollusc shell	NA	2733 ± 30 (71.2 ± 0.3 pMC)	2210 - 2330	260 - 380 BC
633 - 634	AAR-1699	Mollusc shell	NA	2845 ± 37 (70.2 ± 0.3 pMC)	2330 - 2460	380 - 510 BC
691 - 692	Poz-30972	Mollusc shell	NA	2956 ± 30 (69.2 ± 0.3 pMC)	2500 - 2660	550 - 710 BC
740 - 742	Poz-33418	mix benthic forams	NA	3217 ± 34 (67 ± 0.3 pMC)	2780 - 2910	830 - 960 BC
782 - 783	Poz-30973	Mollusc shell	NA	3430 ± 33 (65.2 ± 0.3 pMC)	3060 - 3210	1110 - 1260 BC
856 - 857	Poz-30974	Mollusc shell	NA	3544 ± 32 (64.3 ± 0.3 pMC)	3220 - 3340	1270 - 1390 BC
855 - 857	Poz-33419	mix benthic forams	NA	3541 ± 36 (64.4 ± 0.4 pMC)	3220 - 3340	1270 - 1390 BC
905 - 906	Poz-30975	Mollusc shell	NA	3746 ± 26 (62.7 ± 0.2 pMC)	3440 - 3550	1490 - 1600 BC

899

900

901

902

903

904

905

906 Table 2. Grouping of chilled Atlantic Water species (AtIW) and Arctic Water species
907 (AW).

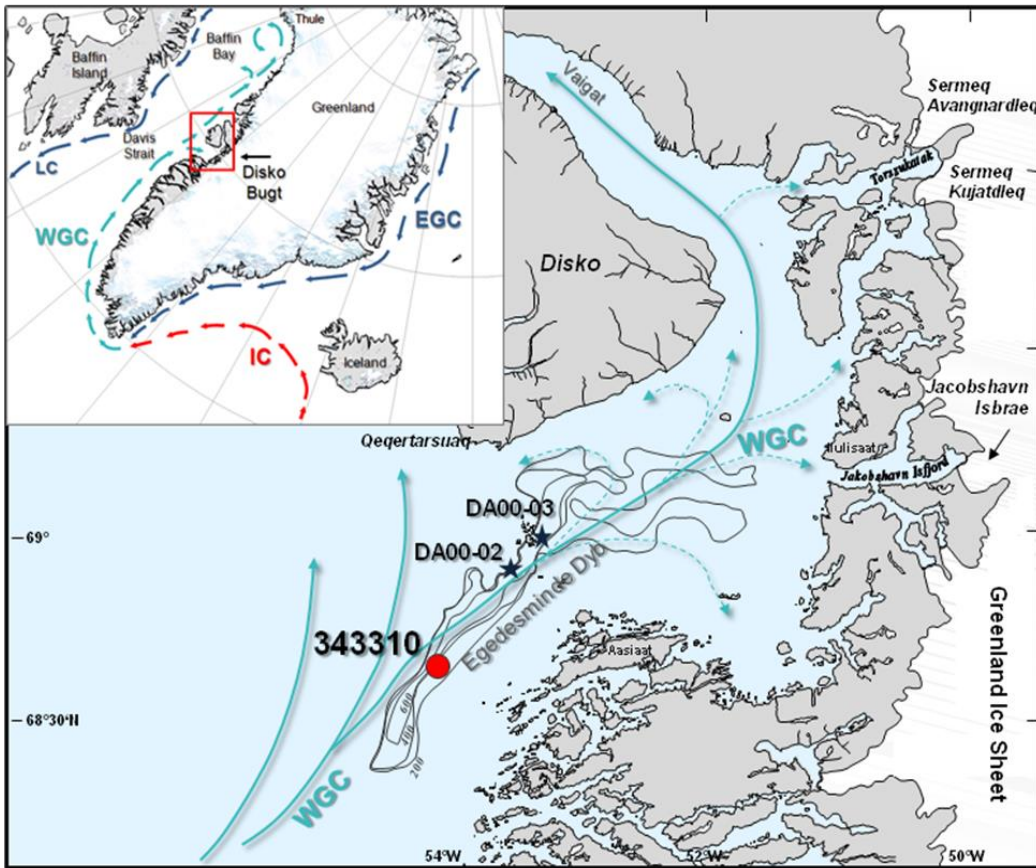
Atlantic Water Species (AtIW)	Arctic Water species (AW)
agglutinated species	
<i>Ammoscalaria pseudospiralis</i>	<i>Cuneata arctica</i>
<i>Reophax fusiformis</i>	<i>Recurvoides turbinatus</i>
<i>Reophax pilulifer</i>	<i>Spiroplectammina biformis</i>
calcareous species	
<i>Cassidulina reniforme</i>	<i>Elphidium excavatum</i> f. <i>clavata</i>
<i>Pullenia osloenesis</i>	<i>Islandiella helenae</i>
<i>Islandiella norcrossi</i>	<i>Stainforthia feylingi</i>

908

909

910 Figures

911 1)



912

913

914

915

916

917

918

919

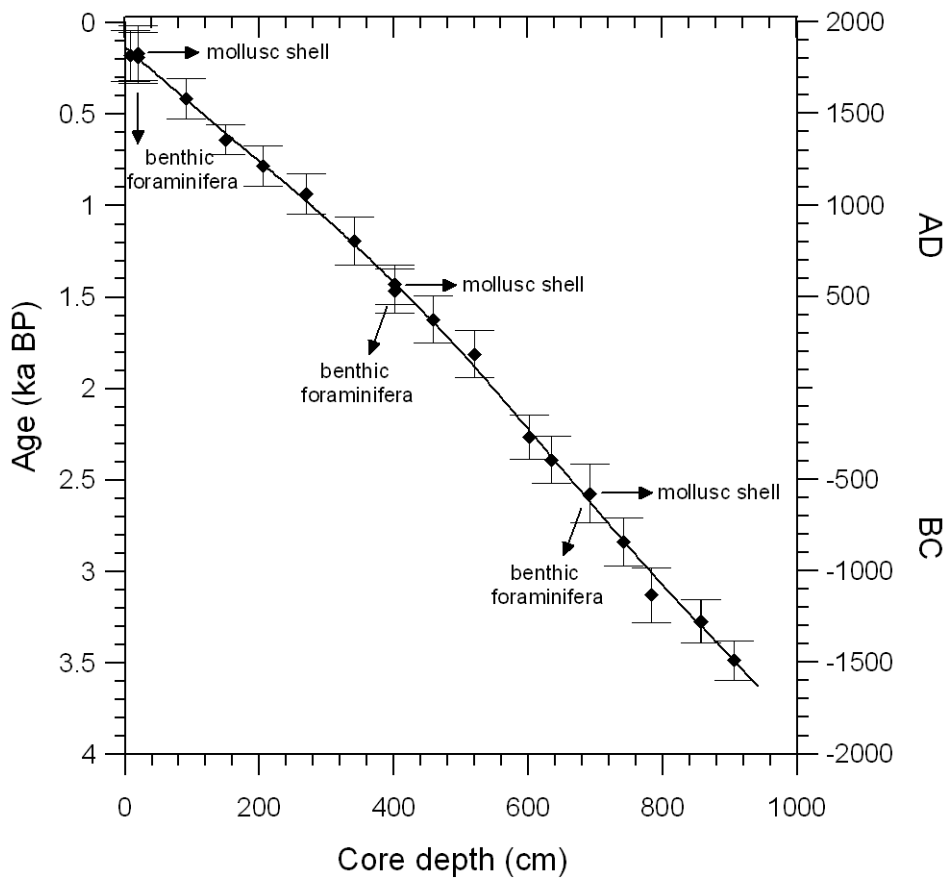
920

921

922

923

924 2)

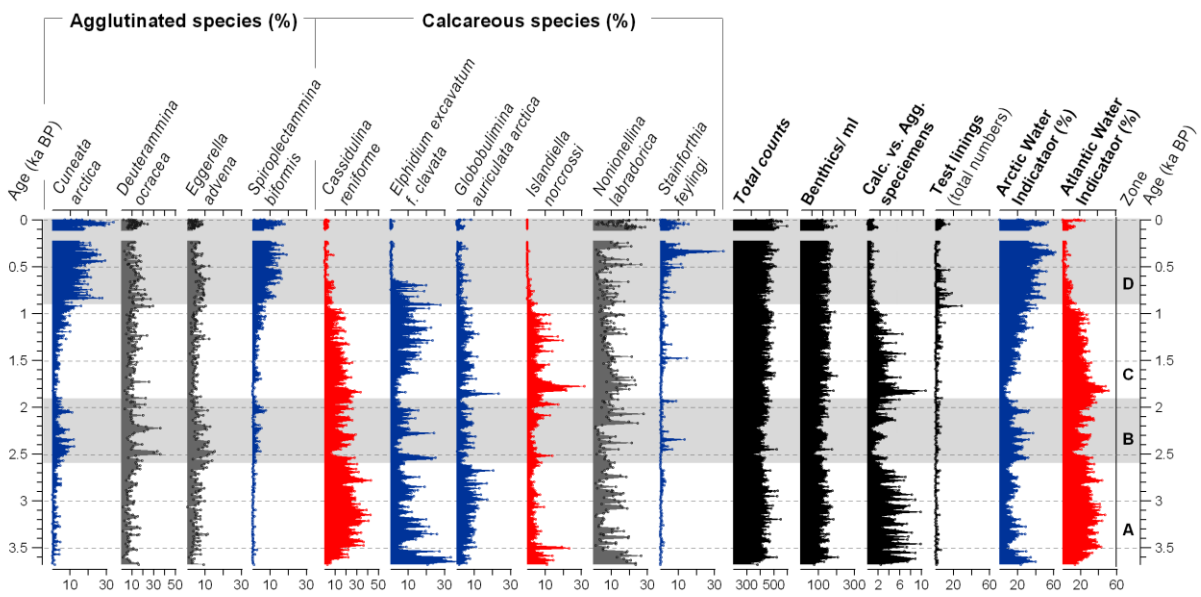


925

926

927

928 3)

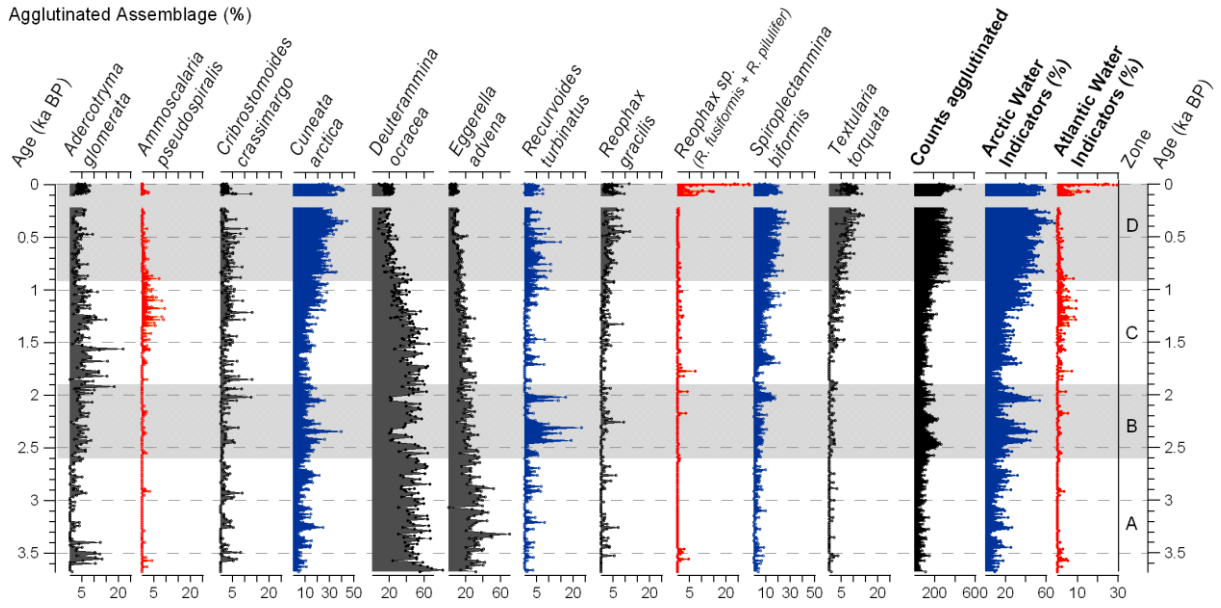


929

930

931 4)

Agglutinated Assemblage (%)



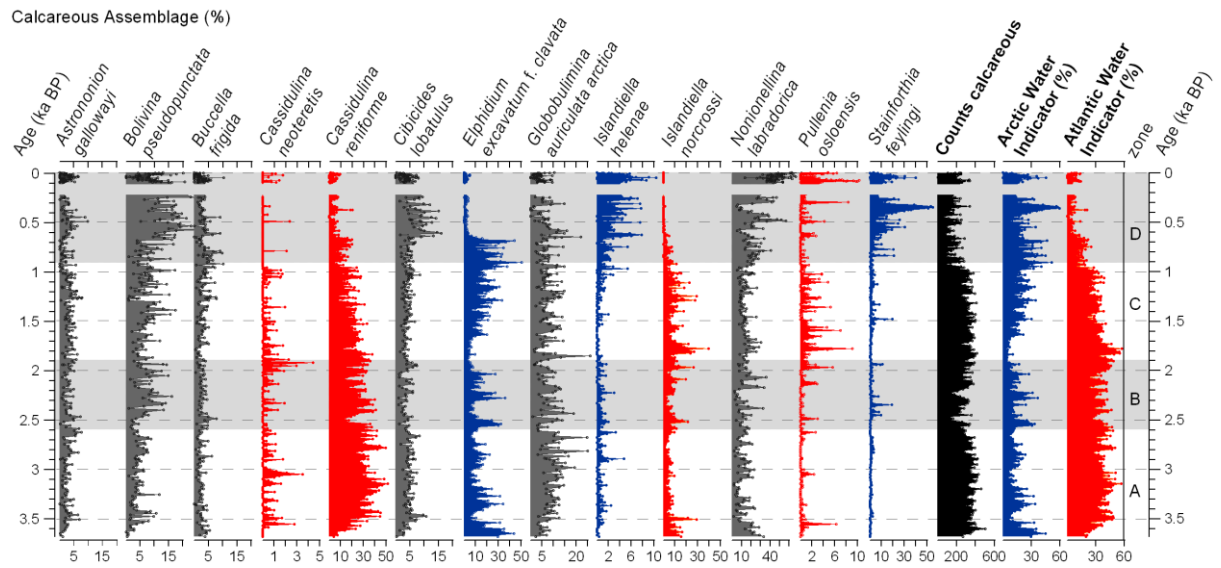
932

933

934

935 5)

Calcareous Assemblage (%)



936

937

938

939

940

941

